Dynamical and Coupling Structure of Pulse-Coupled Networks in Maximum Entropy Analysis

Zhi-Qin John Xu[1],[*] Douglas Zhou[2],[†] and David Cai[1,2,3]

[1]*NYUAD Institute, New York University Abu Dhabi,*
Abu Dhabi, United Arab Emirates,
[2]*School of Mathematical Sciences,*
MOE-LSC and Institute of Natural Sciences,
Shanghai Jiao Tong University, Shanghai, P.R. China,
[3]*Courant Institute of Mathematical Sciences and Center for Neural Science,*
New York University, New York, New York, USA.

Maximum entropy principle (MEP) analysis with few non-zero effective interactions successfully characterizes the distribution of dynamical states of pulse-coupled networks in many experiments, e.g., in neuroscience. To better understand the underlying mechanism, we found a relation between the dynamical structure, i.e., effective interactions in MEP analysis, and the coupling structure of pulse-coupled network to understand how a sparse coupling structure could lead to a sparse coding by effective interactions. This relation quantitatively displays how the dynamical structure is closely related to the coupling structure.

PACS numbers: 89.70.Cf, 87.19.lo, 87.19.ls, 87.19.ll

Binary-state networks—each node in one sampling time bin is binary-state—arise from many research fields, e.g., gene regulatory modeling and neural dynamics [15, 23, 26]. Statistical distributions of network states are essential to encode information [6, 11, 18, 20, 25]. For example, with statistical distributions of network states, experimental studies show that rats can perform awake replays of remote experiences in hippocampus [10]. Many works effectively characterize the distribution of 2^n network states for n binary-state nodes in various systems, e.g., a network of ~ 100 neurons [8], with a *low-order maximum entropy principle* (MEP) analysis [2, 4, 13, 14, 19, 22, 24, 27]—a method with few (far less than 2^n) non-zero effective interactions (see a precise definition in Eq. (1)) constrained by low-order statistics. We can then regard those effective interactions as a sparse coding of the information that encoded in the state distribution. To understand coding schemes of network systems, it is important, however, yet to understand what leads to the sparsity of effective interactions. In this work, we would mainly use neural networks as examples for illustration, while our results apply to general binary-state networks.

Estimated by dynamical data of a network system, effective interactions reflect a dynamical structure of the network. This dynamical structure has been used to study the functional connectivity of networks [7, 27]. For example, experimental studies show that the second-order effective interaction map of the retina is sparse and dominated by local overlapping effective interaction modules [7]. Network dynamical structure often closely relates to the underlying coupling structure [29]. For example, when the input of each node is independent to others, i) high-order (≥ 2) effective interactions are zero in a network of no connections, ii) high-order effective interactions are large in a dense and strong connected excitatory network. To efficiently encode information, a realistic system often incorporates a coupling structure with certain features [3, 17], e.g., sparsity, small-world, or scale-free. However, it is still unclear how the coupling structure affects the dynamical structure of effective interactions.

In this letter, we consider a general class of pulse-coupled networks. The state of each node is binary-state, i.e., active when the node sends pulses to its child nodes, otherwise, silent. We observed a *Fact* that leads to an explicit relation—which is independent of node dynamics—between the coupling structure and the number of non-zero effective interactions in the full-order MEP analysis (constrained by all moments). We examine our observed Fact by numerical simulations. Through our analysis, we can estimate an upper bound of the number of non-zero effective interactions for a given coupling structure when the external input of each node is independent with each other. Our results show that a sparse network could lead to a lot of vanishing high-order effective interactions. For illustration, we estimate the number of non-zero effective interactions for each order in a network with *Erdos-Renyi* connection structure, in which our estimation is much smaller than C_n^k, the number of all possible kth-order effective interactions. Our results establish a connection between the dynamical structure and the network coupling structure. This connection provides an insight into how a sparse coupling structure can lead to a sparse coding scheme.

In the following analysis, we use binary vector $V(l) = (\sigma_1, \cdots, \sigma_n) \in \{0, 1\}^n$ to represent the state of n nodes within the sampling time bin labeled by l. To obtain correlations up to the mth-order requires to evaluate all $\langle \sigma_{i_1} \cdots \sigma_{i_M} \rangle_E$, where $1 \leq i_1 < i_2 < \cdots < i_M \leq n$, $1 \leq M \leq m$, and $\langle \cdot \rangle_E$ is defined by $\langle g(l) \rangle_E = \sum_{l=1}^{N_T} g(l)/N_T$ for any function $g(l)$ and N_T is the total number of sampling time bins in the recording. The mth-order MEP analysis is to find the desired probability distribution $P(V)$ for n nodes by maximizing the entropy $S \equiv -\sum_V P(V) \log P(V)$ subject to correlations up to the mth-order ($m \leq n$). Then, the unique distribution can be solved

---
[*] zhiqinxu@nyu.edu
[†] zdz@sjtu.edu.cn

as

$$P_m(V) = \frac{1}{Z}\exp\Big(\sum_{k=1}^{m}\sum_{i_1<\cdots<i_k}^{n} J_{i_1\cdots i_k}\sigma_{i_1}\cdots\sigma_{i_k}\Big), \qquad (1)$$

where, following the terminology of statistical physics, we call $J_{i_1\cdots i_k}$ a kth-order effective interaction ($1 \le k \le m$), the partition function Z is the normalization factor. Eq. (1) is referred to as the mth-order MEP distribution.

First, we discuss the relationship between effective interactions and the statistical distribution of network states. By taking logarithm of both sides of Eq. (1) for $P_n(V)$, we can get a set linear equations of all-order effective interactions for all states V. Since P_n is the same as the experimental observed distribution [1], we can obtain the effective interactions in P_n in terms of the experimental observed distribution [28]. For example, $n = 3$, we can obtain $J_1 = \log(P_{100}/P_{000})$ and $J_{12} = \log(P_{110}/P_{010}) - J_1$, where $P_{\sigma_1\sigma_2\sigma_3}$ represents the probability of the network state $(\sigma_1,\sigma_2,\sigma_3)$. By applying $P(\sigma_1,\sigma_2,\sigma_3) = P(\sigma_1|\sigma_2,\sigma_3)P(\sigma_2,\sigma_3)$, we have $J_1 = \log\frac{P(\sigma_1=1|\sigma_2=0,\sigma_3=0)}{P(\sigma_1=0|\sigma_2=0,\sigma_3=0)}$ and $J_{12} = \log\frac{P(\sigma_1=1|\sigma_2=1,\sigma_3=0)}{P(\sigma_1=0|\sigma_2=1,\sigma_3=0)} - J_1 \triangleq J_1^1 - J_1$. Our earlier study has shown a recursive structure among effective interactions, that is, the $(k+1)$st-order effective interaction $J_{123\dots(k+1)}$ can be obtained as follows [28]: First, we switch the state of the $(k+1)$st node in $J_{123\dots k}$ from silent to active to obtain a new term $J_{123\dots k}^1$, e.g., from J_1 to J_1^1; Then, we subtract $J_{123\dots k}$ from the new term to obtain $J_{123\dots(k+1)}$, i.e.,

$$J_{123\dots(k+1)} = J_{123\dots k}^1 - J_{123\dots k}. \qquad (2)$$

Without lost of generality, we randomly select two nodes labeled by 1 and 2. By the recursive relation, any kth-order effective interaction that includes node 1 and 2 can be expressed as the summation of terms with the following basic form

$$J_{12}^b(\sigma_3,\cdots,\sigma_n) = \log\frac{P(\sigma_1=1|\sigma_2=1,\sigma_3,\cdots,\sigma_n)}{P(\sigma_1=0|\sigma_2=1,\sigma_3,\cdots,\sigma_n)}$$
$$- \log\frac{P(\sigma_1=1|\sigma_2=0,\sigma_3,\cdots,\sigma_n)}{P(\sigma_1=0|\sigma_2=0,\sigma_3,\cdots,\sigma_n)}. \quad (3)$$

For example, $J_{123} = J_{12}^b(1,0,\cdots,0) - J_{12}^b(0,0,\cdots,0)$ and $J_{1234} = [J_{12}^b(1,1,0,\cdots,0) - J_{12}^b(0,1,0,\cdots,0)] - J_{123}$. We can observe that if nodes 1 and 2 are independent conditioned on all other nodes, i.e., $P(\sigma_1|\sigma_2=1,\sigma_3,\cdots,\sigma_n) = P(\sigma_1|\sigma_2=0,\sigma_3,\cdots,\sigma_n)$, any effective interaction containing these two nodes is zero.

Next, we would show what kind of coupling structure could entail the conditional independence of two nodes. Here, we define some notations. In any sampling time bin $[0,\Delta)$ with state $V = (\sigma_1,\cdots,\sigma_n)$, $\forall t \in [0,\Delta)$, we denote $I_{i,t}$ as node i's input from the outside of the network, denote $w_{ij}(t)$ as the input from the node i to node j, denote $C(i)$ as the set of all child notes of node i, denote $U_i = C(i) \cup \{i\}$, denote $P(e)$ as the probability of event e, denote $U_0 = \{1,2,\cdots,n\}$.

Fact. *For n pulse-coupled nodes with binary-state dynamics on a network with a coupling structure G_0, in any sampling time bin $[0,\Delta)$, $\forall t \in [0,\Delta)$, $\forall i_1, j_1 \in U_0$, we assume that:*

(a) the external inputs of each node are independent to others, i.e., $P(I_{i_1,t}, I_{j_1,t}) = P(I_{i_1,t})P(I_{j_1,t})$; (b) whether a parent node sends spikes to its child nodes only depends on its state, i.e., $P(w_{i_1 j_1}(t), V) = W(\sigma_{i_1}, i_1, j_1, t)$, where $W(\cdot,\cdot,\cdot,\cdot)$ is a real function. $\forall i,j \in U_0$, if they neither are connected nor share any common child node, i.e., $U_i \cap U_j = \phi$, then, node i and j are independent conditioned on the state of all other nodes, i.e.,

$$P(\sigma_i,\sigma_j|H) = P(\sigma_i|H)P(\sigma_j|H), \qquad (4)$$

where H is a possible state of nodes in $U_0\backslash\{i,j\}$.

We justify our two assumptions as follows. To avoid the influence of correlation in external inputs when we are studying the relation between the dynamical structure and the coupling structure, we assume that the external input of each node is independent to others, i.e., assumption (a). The second assumption implicates a Markov-like property; that is, for a connected pair of pulse-coupled nodes in an equilibrium state, the pulse from the parent node to the child node only depends on the state of the parent node but is independent of inputs imposed on the parent node. For example, in neural networks, a neuron sends out spikes only when this neuron is active, regardless of what inputs are imposed on the neuron.

The argument for the conclusion in Eq. (4) is as follows. By assumption (a), node i and node j can be dependent only through the coupling structure G_0. When we are considering how node i and node j affect each other by changing their states through the coupling structure G_0, we can consider a simplified coupling structure, G_1, which ignores those connections that are independent of states of node i and node j, i.e., σ_i and σ_j. $\forall k \in U_o\backslash\{i,j\}$, i.e., any other node k, its state σ_k is fixed when we are considering the conditional probability in Eq. (4). By assumption (b), for node k's any child node l, the input from node k to node l is independent of σ_i and σ_j. Thus, the connections started from those nodes in $U_o\backslash\{i,j\}$ are fixed for different states of σ_i and σ_j. Therefore, G_1 is a simplified coupling structure that only keeps those connections originated from node i and node j in G_0. In G_1, any connection only exists in either sub-network U_i or sub-network U_j. Under the condition $U_i \cap U_j = \phi$, i.e., they neither are connected nor share any common child node, sub-network U_i and sub-network U_j are two isolated sub-networks. σ_i and σ_j cannot affect each other by changing their states through the coupling structure G_1, that is, node i and j are independent conditioned on the states of all other nodes.

Fig.1 displays an example to illustrate our observed Fact. The coupling structure G_0 is shown in Fig.1a. We focus on node 1 and node 2, where they neither are connected nor share any child node. When the state of other nodes (black) are fixed, all outputs from black nodes can be ignored in the simplified coupling structure G_1, as shown in Fig.1b. Node 1 and node 2 respectively belong to two separate sub-networks. Therefore, nodes 1 and node 2 are independent conditioned on the state of all other nodes.

Based on the recursive structure of effective interactions and the observed Fact, we reach the following conclusion: with the two assumptions in the observed Fact, for a group of
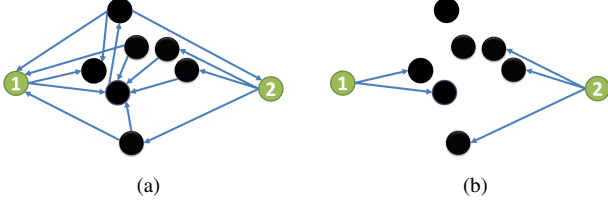
FIG. 1: **Structure v.s. Simplified Structure.**

nodes $\{i_1, i_2, \cdots, i_k\}$, if there exists at least one pair of nodes that neither are connected nor share any child node, effective interaction $J_{i_1, i_2, \cdots, i_k}$ is zero.

In the system we would use to examine our conclusion is an integrate-and-fire (I&F) network, a general pulse-coupled network, with both excitatory and inhibitory nodes [29]. For the ith node, the dynamics of its state variable x_i with time scales τ is governed by

$$\dot{x}_i = -\frac{x_i}{\tau} - (g_i^{\text{bg}} + g^{\text{ex}})(x_i - x_{\text{ex}}) - g_i^{\text{in}}(x_i - x_{\text{in}}), \quad (5)$$

where x_{ex} and x_{in} are the reversal values of excitation (ex) and inhibition (in), respectively. $g_i^{\text{bg}} = f \sum_k \mathbb{H}(t - T_{i,k}^F) \exp[-(t - T_{i,k}^F)/\sigma^{\text{ex}}]$ is the background input with magnitude f and time scale σ^{ex}, $T_{i,k}^F$ is a Poisson process with rate μ, $\mathbb{H}(\cdot)$ is the Heaviside function, $g_i^{\text{ex}} = \sum_j \sum_k S_{ij}^{\text{ex}} \mathbb{H}(t - T_{j,k}^{\text{ex}}) \exp[-(t - T_{j,k}^{\text{ex}})/\sigma^{\text{ex}}]$ is the excitatory pulse effective interaction from other jth excitatory nodes, and $g_i^{\text{in}} = \sum_j \sum_k S_{ij}^{\text{in}} \mathbb{H}(t - T_{j,k}^{\text{in}}) \exp[-(t - T_{j,k}^{\text{in}})/\sigma^{\text{in}}]$ is the inhibitory pulse effective interaction from other jth inhibitory nodes. The jth excitatory (inhibitory) node x_j evolves continuously according to Eq. (5) until it reaches a firing threshold x_{th}. That moment in time is referred to as a firing event (say, the kth spike) and denoted by $T_{j,k}^{\text{ex}}$ ($T_{j,k}^{\text{in}}$). Then, x_j is reset to the reset value x_r ($x_{\text{in}} < x_r < x_{\text{th}} < x_{\text{ex}}$) and held x_r for an absolute refractory period of τ_{ref}. Each spike emerging from the jth excitatory (inhibitory) node causes an instantaneous increase S_{ij}^{ex} (S_{ij}^{in}) in g_i^{ex} (g_i^{in}), where S_{ij}^{ex} and S_{ij}^{in} are the excitatory and inhibitory coupling strengths, respectively. The model (5) describes a general class of physical networks [5, 9, 15, 26, 29].

The first example, two excitatory and two inhibitory I&F nodes form a ring coupling structure (Fig.2a). For any pair of nodes, say, node i and j, we compute $\Delta_{ij}(H) = |P(\sigma_i = 1 | \sigma_j = 1, H) - P(\sigma_i = 1 | \sigma_j = 0, H)|$, where H is one state of other two nodes. By our observed Fact, the conditional independent pairs are (neuron 1, neuron 3) and (neuron 2, neuron 4), and other pairs are categorized as dependent pairs. In Fig.2b, the strengths of $\Delta_{ij}(H)$ of independent pairs (green) are almost two orders of magnitude smaller than those of dependent pairs (red). We then shuffle spike trains of each node. We similarly compute $\Delta_{ij}(H)$ for 10 different shuffled data. Blue dots and cyan dots in Fig.2b are results of all shuffled data of dependent pairs and independent pairs, respectively. The strength of $\Delta_{ij}(H)$ of independent pairs (green)—computed from the observed data—are within the statistical error of shuffled data. We then solve effective interactions in the full-order MEP

analysis P_n for this ring network. As shown in Fig.2c, the effective interaction strengths of independent pairs (J_{24} and J_{13}) are within the statistical error of shuffled results (red). Since every high-order (≥ 3) effective interaction includes at least one independent pair of nodes, as predicted, the strengths of all high-order effective interactions are within the statistical error of shuffled results as shown in Fig.2d.

The second example in the second row in Fig.2, results are similar that dependent pairs and independent pairs can be identified through our observed Fact, and the strength of any effective interaction that includes the independent pair of nodes (node 1 and node 3) is within the statistical error of shuffled data. In this example, J_{124} is very small, i.e., within the statistical error of shuffled results. However, in our estimation by our conclusion, we do not categorized J_{124} to the class of zero-strength effective interactions. This example indicates that we estimate an upper bound of the number of non-zero effective interactions. For a network of all excitatory nodes with the same coupling structure as the one in Fig.1e, J_{124} is significantly larger than zero (not shown). Since the strength of high-order effective interactions is small, a very long recording constraints us from examining $\Delta_{ij}(H)$ for a large network.

Base on the relation between the coupling structure and effective interactions, the number of non-zero high-order effective interactions can be small in a sparse connected network compared with C_n^k, which is the number of all possible kth-order interactions. For example, we estimate the number of each-order non-zero effective interactions in a network with an *Erdos-Renyi* connection structure. We randomly generate 1000 networks of 100 nodes with an *Erdos-Renyi* connection. The connection probability between two nodes is 0.05. As shown in Fig.3, the number of non-zero kth-order ($k > 1$) effective interactions is much smaller than C_{100}^k (too large to be shown). The number of high-order effective interactions (order higher than 11th) almost vanishes (order higher than 20th not shown).

In summary, we have established a relation between effective interactions in MEP analysis and the coupling structure of pulse-coupled networks to understand how a sparse coupling structure could lead to a sparse coding by effective interactions. This relation quantitatively displays how the dynamical structure closely relates to the coupling structure.

Even though high-order effective interactions are often much smaller compared with low-order ones [28], it is still unclear why small high-order effective interactions do not accumulate to have a significant effect in a large network [8, 21]. For example, MEP distribution with a sparse low-order effective interactions—non-zero effective interactions are sparse and vanish when the order is high than the eighth-order—can well capture the state distribution of 99 ganglion cells in the salamander retina responding to a natural movie clip or natural pixel [8]. In this study, we show that a large amount of effective interactions vanish in a sparse coupling structure; thus, rationalizing the absence of the accumulation of high-order interactions for a large network.

Finally, we point out that some important issues remain to be elucidated in the future. First, we have ignored correlations in external inputs when estimating the number of non-zero
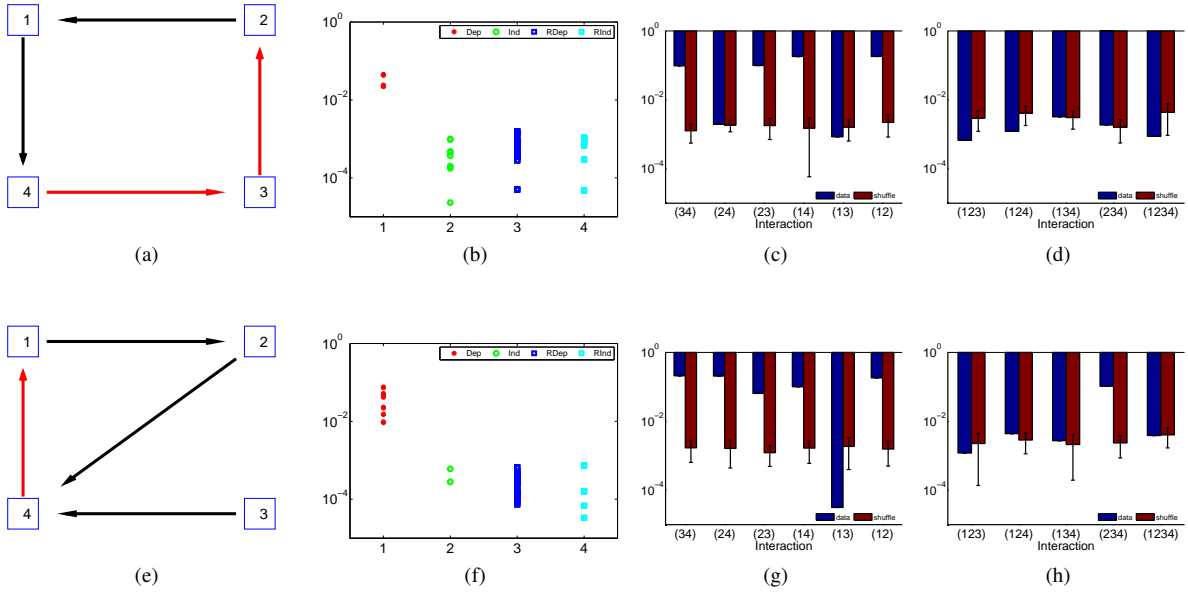
FIG. 2: **Structure v.s. effective interactions of I&F networks .** Each row shows a numerical case. In the first column, black arrows and red arrows represents excitatory and inhibitory connections, respectively. In the second column, red and green dots are the strengths of $\Delta_{ij}(H)$ of dependent and independent pairs, respectively. Blue dots and cyan dots are the strengths of $\Delta_{ij}(H)$ of dependent and independent pairs from ten shuffled spike trains, respectively. The third and fourth columns display absolute effective interaction strengths (blue bars). The corresponding node indexes for each effective interaction are shown in the abscissa. The mean and standard deviation of absolute strengths of each effective interaction of ten shuffled spike trains are also displayed by garnet bars. The simulation time for each network is 1.2×10^8 ms. The time bin size for analysis is 10 ms [22, 24]. Independent Poisson inputs for each network are $\mu = 0.1 \, \mathrm{ms}^{-1}$ and $f = 0.1 \, \mathrm{ms}^{-1}$. The firing rate of each node is about 50 Hz. Parameters are chosen [9] as $x_{\mathrm{ex}} = 14/3$, $x_{\mathrm{in}} = -2/3$, $\sigma^{\mathrm{ex}} = 2$ ms, $\sigma^{\mathrm{in}} = 5$ ms, $\tau = 20$ ms, $x_{\mathrm{th}} = 1$, $x_r = 0$, and $\tau_{\mathrm{ref}} = 2$ ms, $S_{ij}^{\mathrm{ex}} = S_{ij}^{\mathrm{in}} = 0.02$.
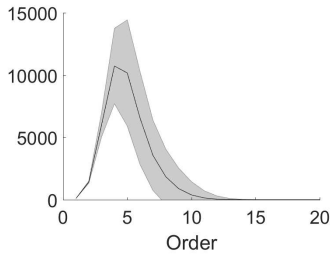

FIG. 3: **Network of Erdos-Renyi connection.** We randomly generate 1000 networks of 100 nodes with an *Erdos-Renyi* connection. The connection probability between two nodes is 0.05. The number of non-zero effective interaction v.s. effective interaction order. The mean and standard deviation are respectively shown by the black line and shaded area.

effective interactions. Correlated inputs can induce non-zero high-order effective interactions [12]. It is yet to consider how the statistics of inputs affect the sparsity of effective interactions. Second, current algorithms for estimating non-zero effective interactions (not limited to the second-order) for a

large network (e.g., ~ 100 nodes) are very slow, e.g., Monte Carlo based methods [16, 21]. Our undergoing work is exploring a fast algorithm that exploits the sparsity of effective interactions. We have seen an indication that the algorithm can work well for an I&F network with sparse coupling structure; however, that work is yet to be fully verified to be conclusive.

[1] S.-I. AMARI, *Information geometry on hierarchy of probability distributions*, Information Theory, IEEE Transactions on, 47 (2001), pp. 1701–1711.

[2] A. K. BARREIRO, J. GJORGJIEVA, F. RIEKE, AND E. SHEA-BROWN, *When do microcircuits produce beyond-pairwise correlations?*, Frontiers in computational neuroscience, 8 (2014).

[3] E. BULLMORE AND O. SPORNS, *Complex brain networks: graph theoretical analysis of structural and functional systems*, Nature Reviews Neuroscience, 10 (2009), pp. 186–198.

[4] T. BURY, *Statistical pairwise interaction model of stock market*, The European Physical Journal B, 86 (2013), p. 89.

[5] D. CAI, A. V. RANGAN, AND D. W. MCLAUGHLIN, *Architectural and synaptic mechanisms underlying coherent spontaneous activity in v1*, Proceedings of the National Academy of Sciences of the United States of America, 102 (2005), pp. 5868–5873.

[6] Y. DAN, J.-M. ALONSO, W. M. USREY, AND R. C. REID, *Coding of visual information by precisely correlated spikes in the lateral geniculate nucleus*, Nature neuroscience, 1 (1998), pp. 501–507.

[7] E. GANMOR, R. SEGEV, AND E. SCHNEIDMAN, *The architecture of functional interaction networks in the retina*, The journal of neuroscience, 31 (2011), pp. 3044–3054.

[8] E. GANMOR, R. SEGEV, AND E. SCHNEIDMAN, *Sparse low-order interaction network underlies a highly correlated and learnable neural population code*, Proceedings of the National Academy of Sciences, 108 (2011), pp. 9679–9684.

[9] W. GERSTNER AND W. M. KISTLER, *Spiking neuron models: Single neurons, populations, plasticity*, Cambridge university press, 2002.

[10] M. P. KARLSSON AND L. M. FRANK, *Awake replay of remote experiences in the hippocampus*, Nature neuroscience, 12 (2009), p. 913.

[11] D. C. KNILL AND A. POUGET, *The bayesian brain: the role of uncertainty in neural coding and computation*, TRENDS in Neurosciences, 27 (2004), pp. 712–719.

[12] J. H. MACKE, M. OPPER, AND M. BETHGE, *Common input explains higher-order correlations and entropy in a simple model of neural population activity*, Physical Review Letters, 106 (2011), p. 208102.

[13] O. MARRE, S. EL BOUSTANI, Y. FRÉGNAC, AND A. DESTEXHE, *Prediction of spatiotemporal patterns of neural activity from pairwise correlations*, Physical review letters, 102 (2009), p. 138101.

[14] E. A. MARTIN, J. HLINKA, AND J. DAVIDSEN, *Pairwise network information and nonlinear correlations*, Physical Review E, 94 (2016), p. 040301.

[15] R. E. MIROLLO AND S. H. STROGATZ, *Synchronization of pulse-coupled biological oscillators*, SIAM Journal on Applied Mathematics, 50 (1990), pp. 1645–1662.

[16] H. NASSER, O. MARRE, AND B. CESSAC, *Spatio-temporal spike train analysis for large scale networks using the maximum entropy principle and monte carlo method*, Journal of Statistical Mechanics: Theory and Experiment, 2013 (2013), p. P03006.

[17] M. E. NEWMAN, *The structure and function of complex networks*, SIAM review, 45 (2003), pp. 167–256.

[18] I. E. OHIORHENUAN, F. MECHLER, K. P. PURPURA, A. M. SCHMID, Q. HU, AND J. D. VICTOR, *Sparse coding and high-order correlations in fine-scale cortical networks*, Nature, 466 (2010), pp. 617–621.

[19] E. SCHNEIDMAN, M. J. BERRY, R. SEGEV, AND W. BIALEK, *Weak pairwise correlations imply strongly correlated network states in a neural population*, Nature, 440 (2006), pp. 1007–1012.

[20] Y. SHEMESH, Y. SZTAINBERG, O. FORKOSH, T. SHLAPOBERSKY, A. CHEN, AND E. SCHNEIDMAN, *High-order social interactions in groups of mice*, Elife, 2 (2013), p. e00759.

[21] J. SHLENS, G. D. FIELD, J. L. GAUTHIER, M. GRESCHNER, A. SHER, A. M. LITKE, AND E. CHICHILNISKY, *The structure of large-scale synchronized firing in primate retina*, The Journal of Neuroscience, 29 (2009), pp. 5022–5031.

[22] J. SHLENS, G. D. FIELD, J. L. GAUTHIER, M. I. GRIVICH, D. PETRUSCA, A. SHER, A. M. LITKE, AND E. CHICHILNISKY, *The structure of multi-neuron firing patterns in primate retina*, The Journal of neuroscience, 26 (2006), pp. 8254–8266.

[23] J. STRICKER, S. COOKSON, M. R. BENNETT, W. H. MATHER, L. S. TSIMRING, AND J. HASTY, *A fast, robust and tunable synthetic gene oscillator*, Nature, 456 (2008), pp. 516–519.

[24] A. TANG, D. JACKSON, J. HOBBS, W. CHEN, J. L. SMITH, H. PATEL, A. PRIETO, D. PETRUSCA, M. I. GRIVICH, A. SHER, ET AL., *A maximum entropy model applied to spatial and temporal correlations from cortical networks in vitro*, The Journal of Neuroscience, 28 (2008), pp. 505–518.

[25] W. E. VINJE AND J. L. GALLANT, *Sparse coding and decorrelation in primary visual cortex during natural vision*, Science, 287 (2000), pp. 1273–1276.

[26] Z. WANG, Y. MA, F. CHENG, AND L. YANG, *Review of pulse-coupled neural networks*, Image and Vision Computing, 28 (2010), pp. 5–13.

[27] T. WATANABE, S. HIROSE, H. WADA, Y. IMAI, T. MACHIDA, I. SHIROUZU, S. KONISHI, Y. MIYASHITA, AND N. MASUDA, *A pairwise maximum entropy model accurately describes resting-state human brain networks*, Nature communications, 4 (2013), p. 1370.

[28] Z.-Q. J. XU, G. BI, D. ZHOU, AND D. CAI, *A dynamical state underlying the second order maximum entropy principle in neuronal networks*, Communications in Mathematical Sciences, 15 (2017), pp. 665–692.

[29] D. ZHOU, Y. XIAO, Y. ZHANG, Z. XU, AND D. CAI, *Causal and structural connectivity of pulse-coupled nonlinear networks*, Physical review letters, 111 (2013), p. 054102.